Supplement of Atmos. Chem. Phys., 22, 4117–4128, 2022
https://doi.org/10.5194/acp-22-4117-2022-supplement

Atmospheric Chemistry and Physics
Open Access
EGU

Supplement of

Direct observations indicate photodegradable oxygenated volatile organic compounds (OVOCs) as larger contributors to radicals and ozone production in the atmosphere

Wenjie Wang et al.

Correspondence to: Bin Yuan (byuan@jnu.edu.cn) and Hang Su (h.su@mpic.de)

1 Calibration of GC-MS

Cylinder standard gases were employed to calibrate the online GC-MS/FID system. A 63-chemicals mixture standard (Spectra Gases) was used to calibrate C2–C6 OVOCs and halocarbons. The calibration curves for each species were acquired by diluting the mixture standard gas into five concentration gradients. The coefficients of determination (r^2) for all calibration curves are larger than 0.995. Ambient concentrations of C2–C6 OVOCs were calculated according to their calibration curves. It is worth noting that these OVOCs may be unstable in cylinders. Additionally, the preconcentration procedures for the GC-MS technique may cause loss of the OVOCs especially under high RH condition because of their relatively high Henry constants. We compared OVOC concentrations measured by GC-MS and PTR-ToF-MS. The measurement results of the two instruments are generally similar (Figure S1). The differences of the two instruments for MVK+MACR, C3H4O and C4H8O are within 20%. However, acetone measured by GC-MS is 46% higher than that measured by PTR-ToF-MS. The differences between GC-MS and PTR-ToF-MS are acceptable, as uncertainties of OVOCs measurements of GC-MS and PTR-ToF-MS are in the range of 20-30%.

Given the higher accuracy of PTR-ToF-MS technology in terms of measuring OVOCs, we gave priority to utilizing the OVOCs data of PTR-ToF-MS for analysis in this study. To reduce the uncertainty of PTR-ToF-MS induced by isomers, the concentrations of acetone were determined by the difference between the C_3H_6O concentrations measured by PTR-ToF-MS and propanal concentrations measured by GC-MS; the concentrations of MVK and MACR were determined according to C_4H_6O concentration measured by PTR-ToF-MS and the ratio of MVK to MACR measured by GC-MS.

2 The influence of measurement uncertainty on the calculation of $P(RO_X)$

The common OVOCs species were calibrated in this study. However, some OVOC species, including pyruvic acid, nitrophenol, methyl nitrophenol and carbonyls with large carbon number, were not calibrated. For these OVOC species, we used the method proposed by Sekimoto, et al. [1] to determine the relationship between VOC

sensitivity and kinetic rate constants for proton transfer reactions of H_3O^+ with VOCs. The fitted line was used to determine the concentrations of those uncalibrated species. Following the discussions in Sekimoto, et al. [1], the uncertainties of the concentrations for uncalibrated species were about 50 %. The uncertainties in the concentrations of these species lead to uncertainties of 0.04~0.23 ppb h^{-1} (1.3%~8.0%) in calculation of P(RO_X). Among these species, $C_nH_{2n-2}O_2$ (n>3) contributes the largest uncertainty, followed by $C_nH_{2n-4}O_2$ (n>3), $C_n H_{2n-4}O_3$ (n>3), $C_nH_{2n-2}O$ (n>3), $C_nH_{2n}O$ (n>5), pyruvic acid, nitrophenol and methyl nitrophenol.

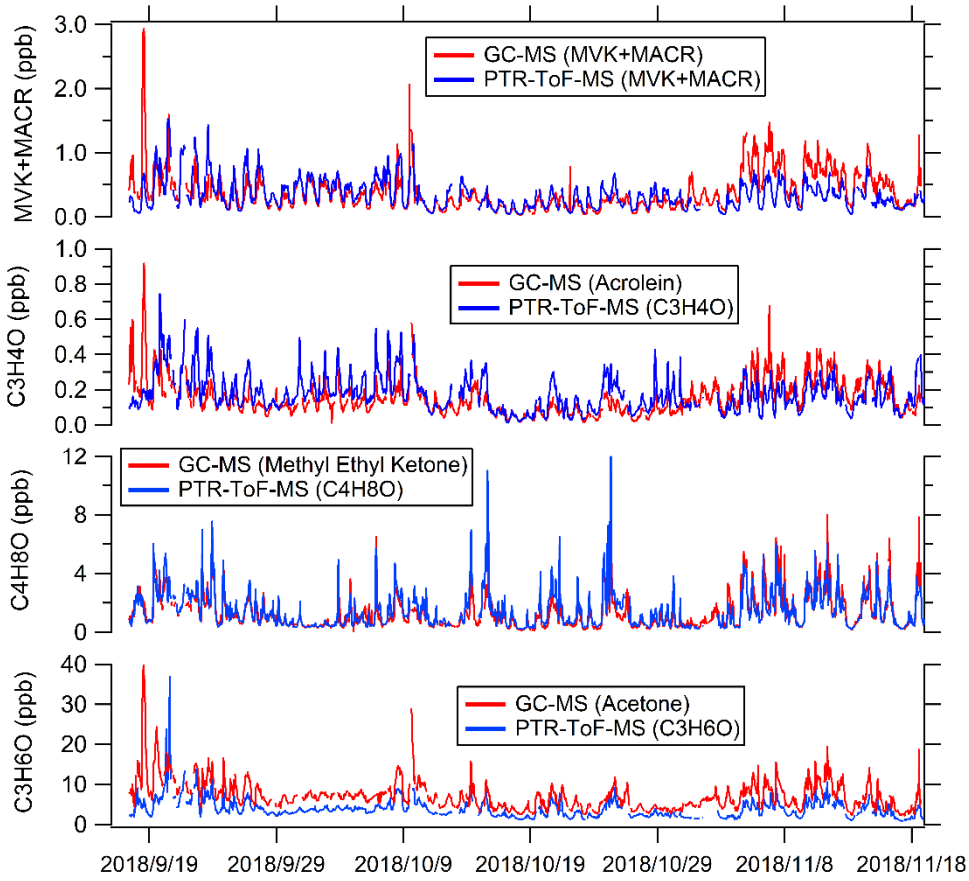

Figure S1. Comparison of typical OVOC concentrations measured by both GC-MS and PTR-ToF-MS.

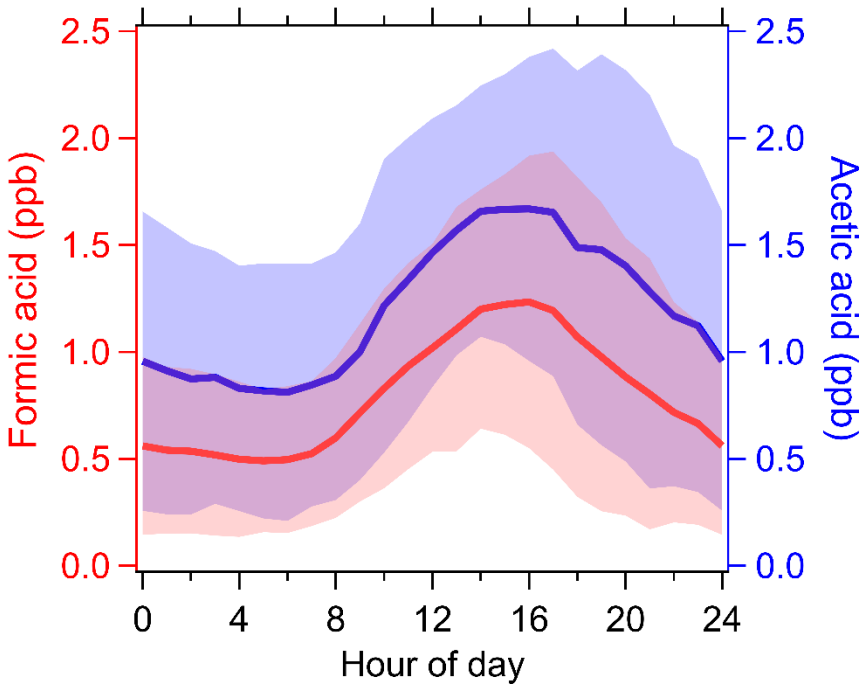

Figure S2. The average diurnal variations of concentrations of formic acid and acetic acid during the campaign.

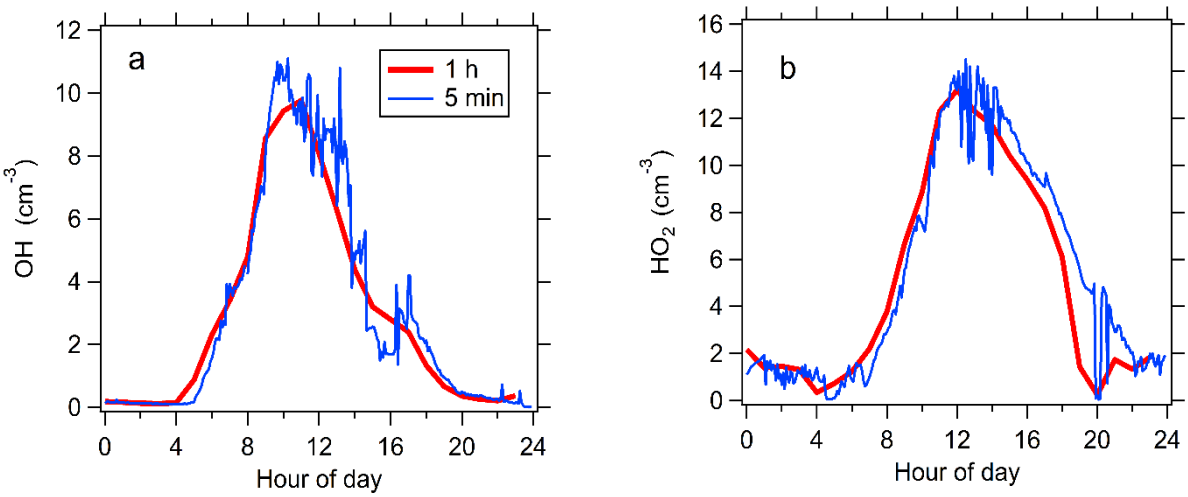

Figure S3. The simulated radical concentrations with 1-h and 5-min time resolution on October 1, 2018.

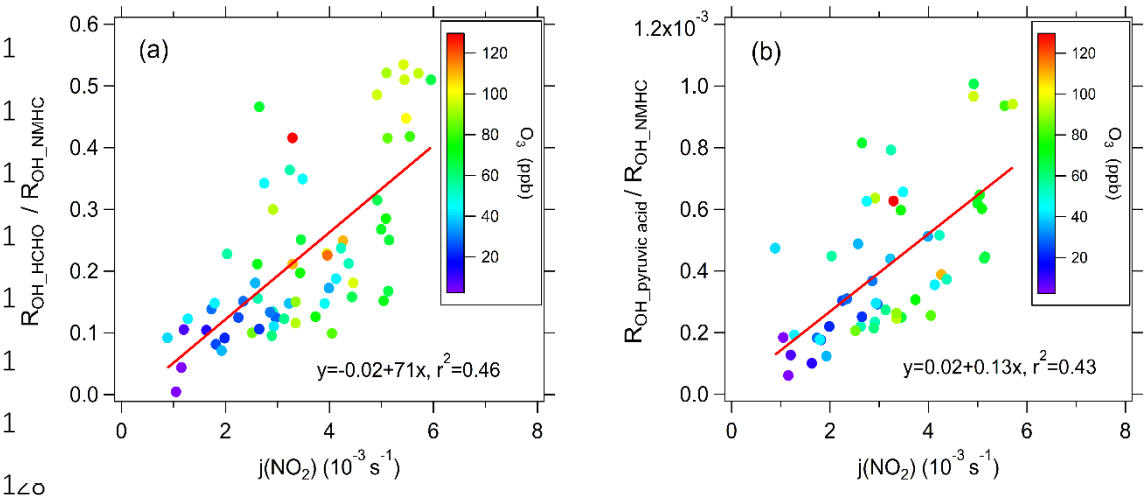

Figure S4. The scatter plot of daily daytime average R_{OH_HCHO}/R_{OH_NMHC} (and $R_{OH\_pyruvic\ acid}/R_{OH\_NMHC}$) ratios versus $j(NO_2)$ color-coded using ozone concentrations during the campaign. Each point corresponds to a daytime average over one day of the campaign.

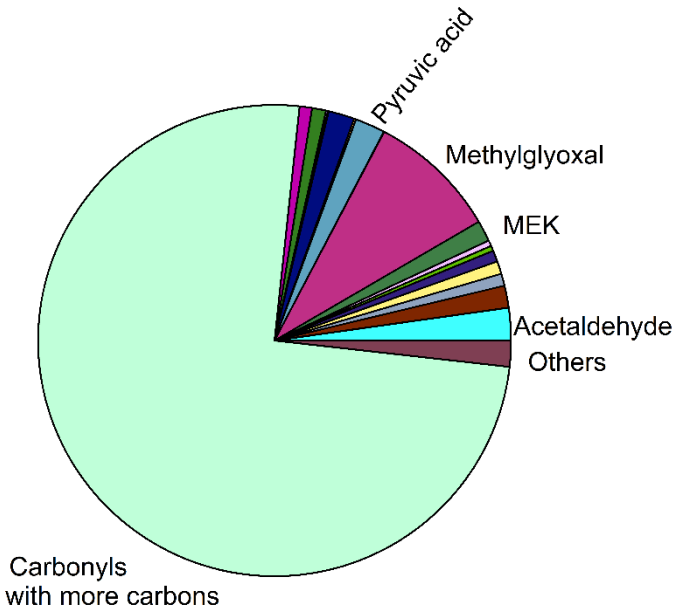

Figure S5. The relative contributions of non-HCHO OVOC species to P(RO_X) for the scenarios with maximum OVOC contribution to P(RO_X).

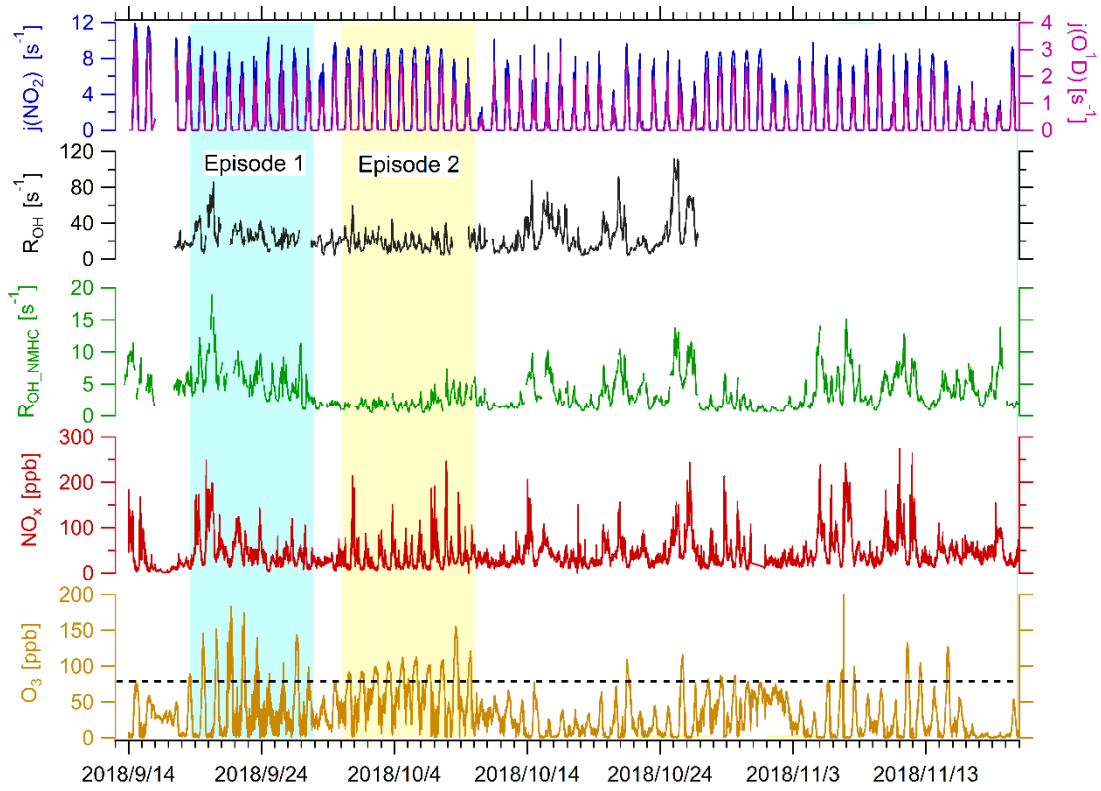

Figure S6. Time series of photolysis frequencies ($j(NO_2)$ and $j(O^1D)$), total OH reactivity (R_{OH}), OH reactivity of NMHCs (R_{OH_NMHC}), NOx concentration and O_3 concentration during the campaign. The blue shade and yellow shade represent the two ozone pollution periods which are defined as episode 1 and episode 2, respectively.

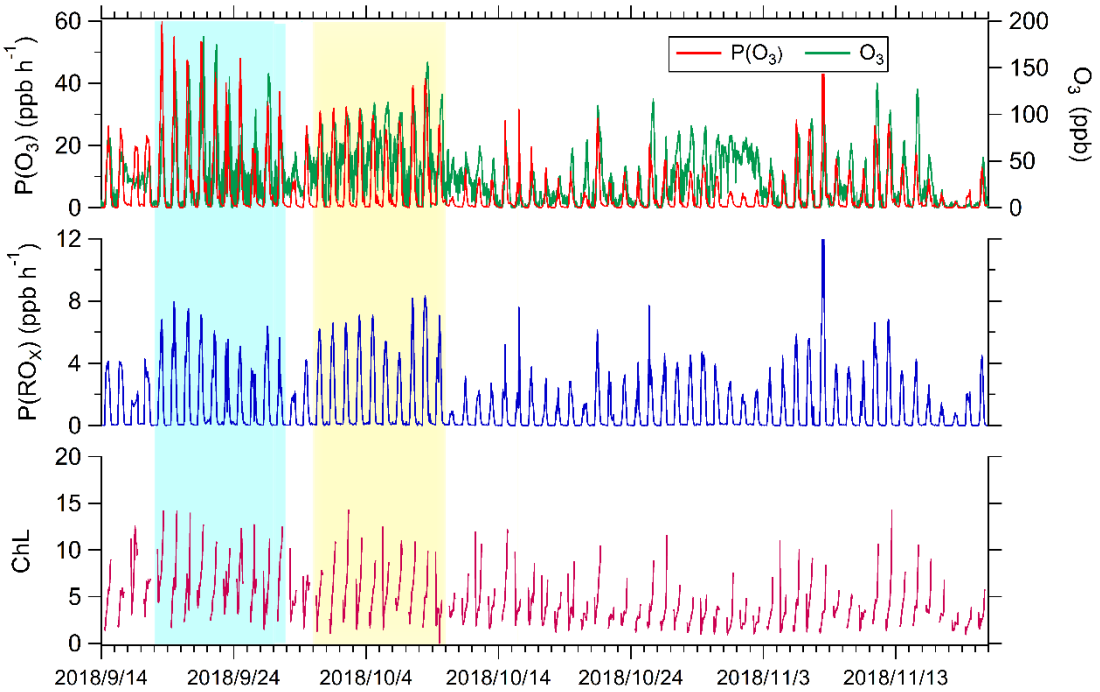

Figure S7. Time series of $P(O_3)$, P(ROx) and ChL during the campaign in Guangzhou. The blue shade and yellow shade represent the two ozone pollution periods which are defined as episode 1 and episode 2 respectively.

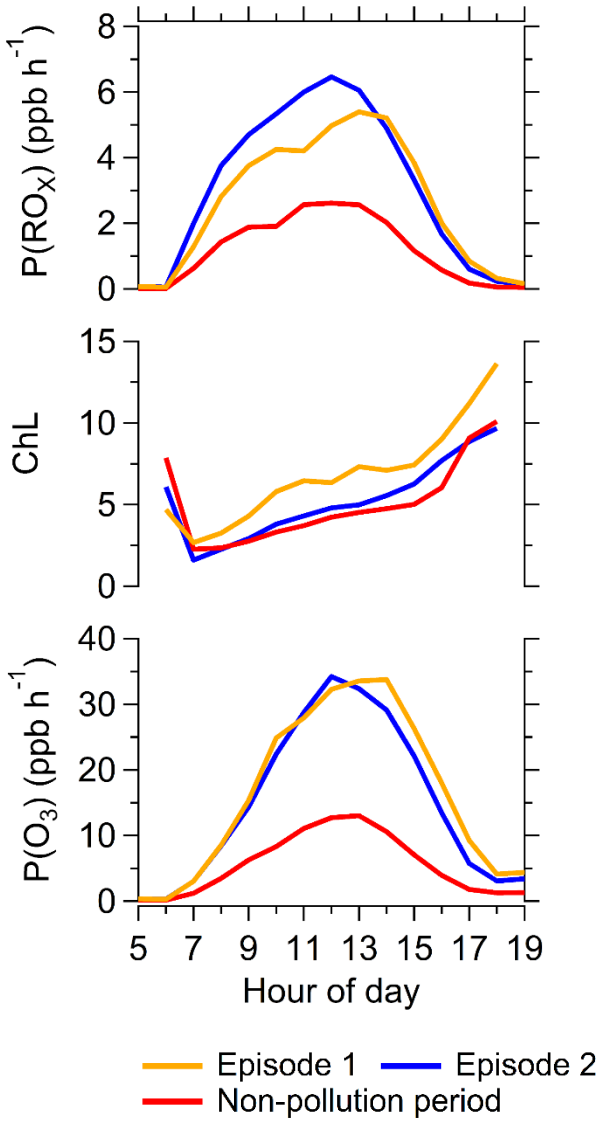

Figure S8. Averaged diurnal variations of P(RO_X), ChL and P(O_3) during episode 1 (yellow line), episode 2 (blue line) and non-pollution period (red line).

197

198 Table S1. Molecular formula, photolysis reactions, daytime average mixing ratio and
199 photolysis frequencies of photodegradable species during the campaign.

Photodegradable species	Molecular formula	Measurement technology	Mixing ratio (ppbv)	Photolysis frequency (s^{-1})
Ozone	O_3	49i O_3 analyzer	48±17	7.0×10^{-6}
Nitrous acid	HONO	LOPAP	0.47±0.20	5.7×10^{-4}
Formaldehyde	HCHO	Hantzsch fluorimetry	5.2±3.8	1.1×10^{-5}
Acetaldehyde	CH_3CHO	GC-MS	2.3±1.2	1.3×10^{-6}
Propanal	C_2H_5CHO	GC-MS	0.35±0.21	6.1×10^{-6}
n-butanal	C_3H_7CHO	GC-MS	0.20±0.14	6.5×10^{-6}
n-pentanal	C4H9CHO	GC-MS	0.21±0.14	6.5×10^{-6}
n-hexanal	C5H11CHO	GC-MS	0.18±0.15	6.7×10^{-6}
Methacrolein	C4H6O	PTR-QiToF-MS, GC-MS	0.22±0.14	1.0×10^{-6}
Acetone	CH_3COCH_3	PTR-QiToF-MS	4.4±2.5	1.4×10^{-7}
Methyl Ethyl Ketone	C_4H_8O	PTR-QiToF-MS	1.8±1.4	1.2×10^{-6}
Methylglyoxal	$C_3H_4O_2$	PTR-QiToF-MS	0.32±0.20	5.5×10^{-5}
Methyl vinyl ketone	C4H6O	PTR-QiToF-MS, GC-MS	0.26±0.15	7.2×10^{-7}
Methyl hydroperoxide	CH_3OOH	PTR-QiToF-MS	0.022±0.015	1.8×10^{-6}
Pyruvic acid	CH_3COCO_2H	PTR-QiToF-MS	0.05±0.04	6.5×10^{-5}
Acrolein	CH_2=CHCHO	PTR-QiToF-MS	0.21±0.10	3.4×10^{-7}
Hydroxyacetone	$CH_3C(O)CH_2OH$	PTR-QiToF-MS	2.0±1.5	1.4×10^{-6}
Hydroxymethyl hydroperoxide	$HOCH_2OOH$	PTR-QiToF-MS	0.06±0.03	1.6×10^{-6}
Benzaldehyde	C7H6O	PTR-QiToF-MS	0.15±0.11	1.0×10^{-6}
Nitrophenol	$C_6H_5NO_3$	PTR-QiToF-MS	0.026±0.018	5.7×10^{-5}
Methyl nitrophenol	$C_7H_7NO_3$	PTR-QiToF-MS	0.023±0.017	5.7×10^{-5}
Carbonyls with more carbons	$C_nH_{2n}O$ (n>5)	PTR-QiToF-MS	0.31±0.24	1.2×10^{-6}~6.5×10^{-6}
	$C_nH_{2n-2}O$ (n>3)	PTR-QiToF-MS	2.04±1.60	1.2×10^{-6}~6.5×10^{-6}
	$C_nH_{2n-2}O_2$ (n>3)	PTR-QiToF-MS	0.42±0.32	1.2×10^{-6}~1.2×10^{-4}
	$C_nH_{2n-4}O_2$ (n>3)	PTR-QiToF-MS	0.20±0.11	1.2×10^{-6}~3.0×10^{-4}
	$C_n H_{2n-4}O_3$ (n>3)	PTR-QiToF-MS	0.13±0.07	1.2×10^{-6}~1.8×10^{-4}

Nitrophenol with more methyl	$C_{6+n}H_{5+2n}NO_3$ ($n \geqslant 1$)	PTR-QiToF-MS	0.021±0.014	5.7×10^{-5}
Benzal with more methyl	$C_{7+n}H_{6+2n}O$ ($n \geqslant 1$)	PTR-QiToF-MS	0.33±0.19	1.0×10^{-6}

200

Table S2. Observed and box-model simulated daytime average concentrations of photodegradable OVOCs and the underestimation fraction of simulation during the campaign.

Photodegradable species	Molecular formula	Observed Concentration (ppbv)	Simulated Concentration (ppbv)	Underestimation of simulation (%)
Formaldehyde	HCHO	5.2±3.8	4.1±3.0	21
Acetaldehyde	CH_3CHO	2.3±1.2	1.5±0.85	35
Propanal	C_2H_5CHO	0.35±0.21	0.25±0.16	29
n-butanal	C_3H_7CHO	0.20±0.14	0.048±0.035	76
n-pentanal	C4H9CHO	0.21±0.14	0.029±0.021	86
n-hexanal	C5H11CHO	0.18±0.15	0.0034±0.0030	98
Methacrolein	C4H6O	0.22±0.14	0.29±0.22	-32
Acetone	CH_3COCH_3	4.4±2.5	1.3±1.1	70
Methyl Ethyl Ketone	C_4H_8O	1.8±1.4	0.38±0.29	79
Methylglyoxal	$C_3H_4O_2$	0.31±0.20	0.20±0.16	35
Methyl vinyl ketone	C4H6O	0.26±0.15	0.34±0.30	-31
Methyl hydroperoxide	CH_3OOH	0.022±0.015	0.016±0.013	27
Pyruvic acid	CH_3COCO_2H	0.05±0.04	0.026±0.022	48
Acrolein	CH_2=CHCHO	0.21±0.10	0.005±0.004	97
Hydroxyacetone	$CH_3C(O)CH_2OH$	2.0±1.5	0.66±0.54	67
Hydroxymethyl Hydroperoxide	$HOCH_2OOH$	0.06±0.03	0.02±0.01	67
Benzaldehyde	C7H6O	0.15±0.11	0.11±0.09	27
Nitrophenol	$C_6H_5NO_3$	0.026±0.018	0.022±0.020	15
Methyl nitrophenol	$C_7H_7NO_3$	0.023±0.017	0.021±0.018	8.7
Carbonyls with more carbons	$C_nH_{2n}O$ (n>5)	0.31±0.24	0.11±0.08	65
	$C_nH_{2n-2}O$ (n>3)	2.04±1.60	0.52±0.37	75
	$C_nH_{2n-2}O_2$ (n>3)	0.42±0.32	0.11±0.07	74
	$C_nH_{2n-4}O_2$ (n>3)	0.20±0.11	0.035±0.26	83
	$C_n H_{2n-4}O_3$ (n>3)	0.13±0.07	0.031±0.022	74
Nitrophenol with more methyl	$C_{6+n}H_{5+2n}NO_3$ (n⩾1)	0.021±0.014	0.011±0.009	48

Benzal with more methyl	$C_{7+n}H_{6+2n}O$ (n⩾1)	0.33±0.19	0.13±0.08	61

204

205

206

Table S3. Daytime (6:00-19:00) average of O_3, $j(NO_2)$, NOx, total OH reactivity (R_{OH}), OH reactivity of NMHCs (R_{OH_NMHC}), and R_{OH_NMHC}/ NOx for the two ozone episodes, other periods, and the campaign average.

Parameter	episode 1	episode 2	Other periods	campaign average
MDA1 O_3 (ppbv)	114±35	106±33	62±22	75±26
MDA8 O_3 (ppbv)	84±27	96±31	48±17	60±19
$j(NO_2)$ (s^{-1})	0.0037±0.0028	0.0053±0.0041	0.0031±0.0025	0.0034±0.0026
NOx (ppbv)	41±27	21±14	37±21	32±17
R_{OH_NMHC} (s^{-1})	6.0±2.8	2.0±0.63	3.2±1.4	3.6±1.6
R_{OH} (s^{-1})	26±16	16±8.0	/	/
R_{OH_NMHC}/ NOx (s^{-1} ppb^{-1})	0.15±0.10	0.095±0.065	0.086±0.055	0.11±0.067

Reference:

1. Sekimoto, K.; Li, S.-M.; Yuan, B.; Koss, A.; Coggon, M.; Warneke, C.; de Gouw, J., Calculation of the sensitivity of proton-transfer-reaction mass spectrometry (PTR-MS) for organic trace gases using molecular properties. *International Journal of Mass Spectrometry* **2017,** *421*, 71-94.